



Mechanism of Reaction in NaAlCl₄ Molten Salt Batteries with Nickel Felt Cathodes and Aluminum Anodes. Part I: Modelling of the Battery Properties at Thermodynamic Equilibrium.

Knutz, B.C.; Hjuler, Hans Aage; Berg, Rolf W.; Bjerrum, Niels

Published in:
Journal of The Electrochemical Society

Link to article, DOI:
[10.1149/1.2221098](https://doi.org/10.1149/1.2221098)

Publication date:
1993

Document Version
Publisher's PDF, also known as Version of record

[Link back to DTU Orbit](#)

Citation (APA):
Knutz, B. C., Hjuler, H. A., Berg, R. W., & Bjerrum, N. (1993). Mechanism of Reaction in NaAlCl₄ Molten Salt Batteries with Nickel Felt Cathodes and Aluminum Anodes. Part I: Modelling of the Battery Properties at Thermodynamic Equilibrium. *Journal of The Electrochemical Society*, 140(12), 3374-3379.
<https://doi.org/10.1149/1.2221098>

General rights

Copyright and moral rights for the publications made accessible in the public portal are retained by the authors and/or other copyright owners and it is a condition of accessing publications that users recognise and abide by the legal requirements associated with these rights.

- Users may download and print one copy of any publication from the public portal for the purpose of private study or research.
- You may not further distribute the material or use it for any profit-making activity or commercial gain
- You may freely distribute the URL identifying the publication in the public portal

If you believe that this document breaches copyright please contact us providing details, and we will remove access to the work immediately and investigate your claim.

14. D. Pavlov and Z. Dinev, *This Journal*, **127**, 855 (1980).
15. E. M. L. Valeriotte and L. D. Gallop, *ibid.*, **124**, 370 (1977).
16. P. Ruetschi and R. T. Angstadt, *ibid.*, **111**, 1323 (1964).
17. D. Pavlov, *Electrochim. Acta*, **13**, 2051 (1968).
18. D. Pavlov, C. N. Poulieff, E. Klaja, and N. Jordanov, *This Journal*, **116**, 316 (1969).
19. M. N. C. Ijomah, *ibid.*, **134**, 2960 (1987).
20. Y. Guo, *J. Electroanal. Chem.*, **323**, 117 (1992).
21. Y. Guo, J. Yue, and C. Liu, *Electrochim. Acta*, **38**, 1131 (1993).
22. H. R. Thirsk and J. A. Harrison, *A Guide to the study of Electrode Kinetics*, p. 61, Academic Press, London (1972).

Mechanism of Reaction in NaAlCl₄ Molten Salt Batteries with Nickel Felt Cathodes and Aluminum Anodes

I. Modeling of the Battery Properties at Thermodynamic Equilibrium

B. C. Knutz,^a H. A. Hjuler,* R. W. Berg, and N. J. Bjerrum*

Materials Science Group, Chemistry Department A, The Technical University of Denmark, DK-2800 Lyngby, Denmark

ABSTRACT

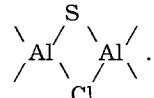
A theoretical description of the thermodynamic properties of the battery systems: Al/NaCl-AlCl₃-Al₂X₃/Ni-felt (X = S, Se, Te) and the corresponding system without chalcogen has been provided for cells with basic to slightly acidic NaCl-AlCl₃ melts containing small amounts of chalcogen. The model developed describes the equilibrium concentrations of constituent species in the electrolyte and equilibrium potentials of the electrodes *vs.* number of coulombs passed through the cells. For cells without chalcogen curves were calculated under the assumption of NiCl₂ formation showing corresponding variation of anode potential, cathode potential, and cell voltage as a function of electrolyte composition. For sulfide containing cells the plateau of lowest potential has been found to be associated with essentially pure nickel sulfide, Ni_yS_z. A procedure for model fitting to the cathode potential curve-form of the Ni_yS_z-plateau is presented. A general equation is proposed for the reaction taking place along the second plateau.

We have previously¹ studied the cycling performance of batteries based on the system Al/NaCl-AlCl₃/Me_yS_z (175°C), where Me_yS_z is a transition metal sulfide, attached to a nickel net current collector.

In this work we present a model describing the equilibrium reactions taking place in similar cells consisting of a pure nickel metal felt cathode in contact with the NaCl-AlCl₃ melt, eventually containing dissolved chalcogens.

The description of the thermodynamic properties of the NaCl-AlCl₃-Al₂X₃ (X = chalcogen) melts forms a basic part of the model. The species and the equilibria in the NaCl-AlCl₃ molten salt have been investigated by several authors.²⁻⁵ Methods like potentiometry, Raman spectroscopy, and vapor pressure measurements have been applied. According to these investigations molten NaCl-AlCl₃ consists essentially of the species Na⁺, AlCl₄⁻, Al₂Cl₇⁻, Cl⁻, Al₃Cl₁₀, Al₂Cl₆, and AlCl₃ in the range of composition between *ca.* 50 and 70 mole percent (m/o) AlCl₃.

Knowledge on how chalcogens exist in chloroaluminate melts seems to be considerably more limited. Previously we studied sulfide containing NaCl-AlCl₃ melts by Raman spectroscopy.⁶ From this work we could conclude that dissolved sulfide most probably exists in the form of ions like Al_nS_{n-1}Cl_{2n+2-m}^{(n-m)-} (2 ≤ n, 0 ≤ m < n), where n is the degree of polymerization and m the number of sulfide-chloride dou-

ble bridges of the type . This configuration

seems to be stable only in acidic melts (>50 m/o AlCl₃) where m attains high values. In basic melts, characterized by an excessive chloride concentration, the sulfide species become saturated with chloride, *i.e.*, m = 0.

The higher chalcogens in NaCl-AlCl₃ probably exist as ions analogous to the sulfide species.⁶ Further, our previ-

ous⁷ measurement of the mass density of NaCl-AlCl₃-Al₂S₃ melts is important for an accurate description of the melt.

In Part II,⁸ calculations based on the model are compared with experimental data. Some of the results obtained from the comparison are reported in this paper to give a connected presentation of the modeling and the results obtained by means of the model. Part II further contains a study of the reaction mechanism by means of Raman spectroscopy on the electrolyte, applied as a function of the degree of charge and discharge, and by means of gravimetric analysis of the electrolyte.

Idealized Equilibrium Open-Circuit Voltage

An idealized equilibrium open-circuit voltage curve for chalcogen containing cells is shown in Fig. 1. Cycling experiments and coulometric titrations, presented in Part II, Ref. 8 reveal at least four major "horizontal" plateaus. Since the anode reaction remains unchanged during charging the different plateaus reflect changes in the cathode reaction. The main charging and discharging regime of cells without chalcogen proceeds at plateau No. 2, which is associated with formation/decomposition of NiCl₂. Plateau No. 1 is not present in this case and only small indications for plateau No. 3 are observed. This shows that the chalcogens are chemically active in the cathode reactions along the plateaus No. 1 and No. 3. From comparison of the performed coulometric titrations on the systems Al/NaCl-AlCl₃-Al₂X₃/Ni-felt (X = S, Se) with theoretical calculations based on the model, we have found that plateau No. 1 involves formation/decomposition of essentially Ni_yS_z in the sulfide system and Ni_ySe_z in the selenide system. The intermediate plateau, No. 2, at ~0.975 V is associated with NiCl₂ or a Ni_yS_zCl_{2y-2z}-type compound. The reaction taking place along plateau No. 3 probably involves an oxidized compound containing chalcogen and nickel.⁸ Plateau No. 4 is associated with decomposition of the NaCl-AlCl₃ melt involving formation of Cl₂.

The position of the plateaus depends on melt composition (acid/base properties) as predicted by the model and observed experimentally. Figure 1 is valid for basic melts.

* Electrochemical Society Active Member.

^a Present address: Randersgade 11, 2. th., DK-2100 København ø, Denmark.

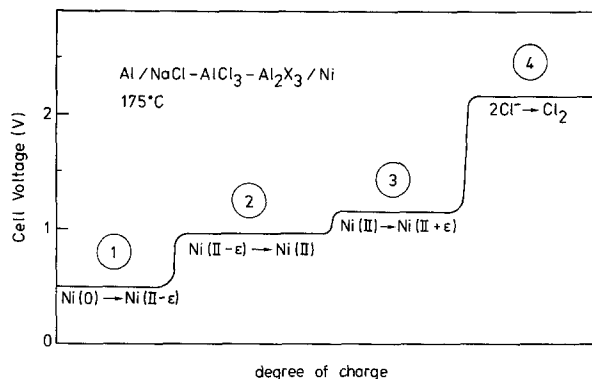


Fig. 1. Idealized equilibrium open-circuit voltage for Al/NaCl-AlCl₃-Al₂X₃/Ni battery cells (X = S, Se, Te) with basic melts at 175°C. Plateaus are labeled No. 1, No. 2, No. 3, and No. 4, according to the description in the text (ε designates the deviation of the average nickel oxidation state from state II). For batteries without chalcogen plateau No. 1 does not occur.

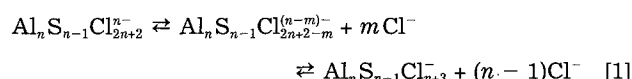
Model

The developed model is presented assuming sulfide containing melts. The changes necessary to cover the systems with higher chalcogens are easily made; see below.

The model describes the variation in equilibrium concentrations of the constituent components of the electrolyte and the variation in equilibrium potentials of anode and cathode as a function of charging and discharging under the assumption of probable cathode reactions. The model consists of a set of equations describing the equilibrium concentrations of the species in the melt as a function of the overall composition of the melt specified by the mole fractions of the formal species NaCl, AlCl₃, and Al₂S₃. To make it complete the model further contains equations specifying the changes in the melt due to electrode reactions and equations for the electrode potentials.

Modeling of the Melt

Several equilibria between the constituent species of the NaCl-AlCl₃-Al₂S₃ melt have to be taken into account when setting up an appropriate mathematical model covering a broad composition range. Unfortunately, equilibria involving the sulfide containing species are at present not well known, particularly with respect to the changes in the degree of polymerization and the release/uptake of chloride. The latter probably proceeds according to the following reactions



assuming no change in polymerization (2 ≤ n, 0 ≤ m < n). However, the equilibria constants are not known.

In order to be able to compare experimental results with theory we used only a small amount of dissolved sulfide and performed the experiments such that only minor changes in the NaCl-AlCl₃ composition occurred. Hence, it seems reasonable to leave out any equilibria involving sulfide and to allow for the presence of only one type of sulfide species (i.e., one set of n, m) in the model. Therefore, the following model should be valid only for systems containing small amounts of dissolved sulfide, and provided the composition of the melt is changed only slightly.

The "acid/base" properties⁴ of the NaCl-AlCl₃ solvent is taken into account by means of the following two equilibria 2 and 3. For compositions below 0.52 m/o AlCl₃ (as is the case in the present work) these two equilibria are sufficient in order to obtain a good mathematical description



K₁ and K₂ are the equilibrium constants at 175°C. Other species such as Al₃Cl₁₀ and AlCl₃ are assumed to be negligible. Equations 2 and 3 together with the following five Eq. 4 through 8 constitute (under the assumptions made above) a complete model describing the composition of the NaCl-AlCl₃-Al₂S₃ melt at equilibrium.

Charge conservation

$$[\text{AlCl}_4^-] + [\text{Al}_2\text{Cl}_7^-] + [\text{Cl}^-] + (n-m)[\text{Al}_n\text{S}_{n-1}\text{Cl}_{2n+2-m}^{(n-m)-}] = [\text{Na}^+] \quad [4]$$

Aluminum conservation

$$[\text{AlCl}_4^-] + 2[\text{Al}_2\text{Cl}_7^-] + 2[\text{Al}_2\text{Cl}_6] + n[\text{Al}_n\text{S}_{n-1}\text{Cl}_{2n+2-m}^{(n-m)-}] = (2n_{\text{Al}_2\text{S}_3} + n_{\text{AlCl}_3}) \frac{[\text{Na}^+]}{n_{\text{NaCl}}} = \left(2 \cdot \frac{X_{\text{Al}_2\text{S}_3}}{X_{\text{NaCl}}} + \frac{X_{\text{AlCl}_3}}{X_{\text{NaCl}}} \right) [\text{Na}^+] \quad [5]$$

Sulfide conservation

$$(n-1)[\text{Al}_n\text{S}_{n-1}\text{Cl}_{2n+2-m}^{(n-m)-}] = 3n_{\text{Al}_2\text{S}_3} \frac{[\text{Na}^+]}{n_{\text{NaCl}}} = 3 \cdot \frac{X_{\text{Al}_2\text{S}_3}}{X_{\text{NaCl}}} [\text{Na}^+] \quad [6]$$

Mass conservation

$$[\text{Na}^+] \left(M_{\text{NaCl}} + \frac{X_{\text{AlCl}_3}}{X_{\text{NaCl}}} M_{\text{AlCl}_3} + \frac{X_{\text{Al}_2\text{S}_3}}{X_{\text{NaCl}}} M_{\text{Al}_2\text{S}_3} \right) = \rho \quad [7]$$

Mass density

$$\rho = 1.693 - 7.38 \cdot 10^{-4} (t - 175) + 0.42 (X_{\text{NaCl}})^{-0.5} + 7.9 (X_{\text{NaCl}})^{-0.5})^2 + 1.17 X_{\text{Al}_2\text{S}_3} \quad (\rho \text{ in g cm}^{-3}, t \text{ in } ^\circ\text{C}) \quad [8]$$

The overall composition of the melt is specified by the formal number of moles n_{NaCl}, n_{AlCl₃}, and n_{Al₂S₃}, or by the formal mole fractions X_{NaCl}, X_{AlCl₃}, and X_{Al₂S₃} for NaCl, AlCl₃, and Al₂S₃, respectively. M_{NaCl}, M_{AlCl₃}, and M_{Al₂S₃} designate molar masses. Square brackets are used to indicate concentrations. In Eq. 5 through 7 the relation, [Na⁺] = n_{NaCl}/volume, was used to eliminate the volume of the molten salt. The expression 8 for the mass density, ρ, was obtained in a previous work,⁷ and is valid for 175°C ≤ t ≤ 350°C, 0.48 ≤ X_{NaCl} ≤ 0.52 and 0 ≤ X_{Al₂S₃} ≤ 0.04 with a precision of ±0.0037 g cm⁻³.

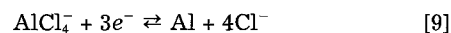
Dissolved selenide in sodium tetrachloroaluminate melts probably exists as ions analogous to the sulfide species of comparable sizes. Therefore, the given model should be applicable for the selenide case too, if only the factor 1.17 in Eq. 8 is substituted by 2.88, taking into account the difference in atomic mass of selenium and sulfur. Corresponding changes should be made to cover melts with dissolved tellurium.

To complete the model, Eq. 2 to 8 should be extended with expressions specifying (i) the changes in the composition of the melt as a function of the degree of electrode reactions and (ii) the relations between properties of the melt and equilibrium potentials of the electrodes. To this end we need to know or postulate the electrode reactions.

It is appropriate to treat the battery system without chalcogen and those containing chalcogen separately.

Chalcogen-Free Cells

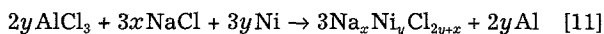
The overall reactions at the aluminum anode can be written



At the cathode we assume formation of a general Na_xNi_yCl_{2y+x} compound (containing divalent Ni) during charging for the following reasons: based on the general chemistry of nickel, formation of Ni(I)-compounds is not likely. Also the possibility that aluminum enters into the formed compound seems unlikely. Accordingly, it has been found in this work (Part II, Ref. 8) and by other investigators⁹ that NiCl₂ is formed at the cathode during charging. Yet, we assume a general Na_xNi_yCl_{2y+x} compound to be able to compare model calculations with experimental results in a systematic way and to account for consumption of NaCl. Therefore, the general cathode reaction during charging can be written



NiCl_2 is obtained if $x = 0$ and $y = 1$. Combining Eq. 9 and 10, the total cell reaction becomes



The changes in the composition of the melt is therefore given by

$$n_{\text{NaCl}} = n_{\text{NaCl}}^0 - \frac{x}{2y} n_e \quad n_{\text{AlCl}_3} = n_{\text{AlCl}_3}^0 - n_e/3; \quad n_{\text{Al}_2\text{O}_3} = 0 \quad [12]$$

Superscript "o" designates initial values, and n_e is the number of "Faradays" (measured positive on charge) passed through the cell.

The potentiometric measurements were performed by means of cells containing an aluminum reference electrode (immersed in NaAlCl_4 melt saturated with NaCl) connected to the real cell compartment through a porous ceramic Al_2O_3 -pin, see Part II, Fig. 1b. Accordingly, the given electrode potentials are stated relative to the aluminum reference electrode. By means of the Nernst law the equilibrium potentials of the anode, E_A , and cathode, E_C , can be expressed by the Eq. 13 and 14

$$E_A = \frac{RT}{3F} \ln \left(\frac{[\text{AlCl}_4^-][\text{Cl}^-]_{\text{ref}}^4}{[\text{AlCl}_4^-]_{\text{ref}}[\text{Cl}^-]^4} \right) = E_A^* + \frac{RT}{3F} \ln \left(\frac{[\text{AlCl}_4^-]}{[\text{Cl}^-]^4} \right) \quad [13]$$

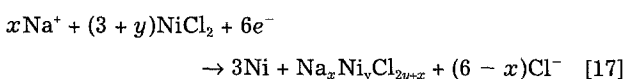
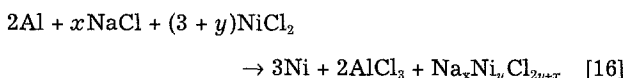
$$E_C = E^* + \frac{RT}{3F} \ln \left(\frac{[\text{Cl}^-]_{\text{ref}}^4}{[\text{AlCl}_4^-]_{\text{ref}}[\text{Na}^+]^{3x/2y}[\text{Cl}^-]^{3+3x/2y}} \right) \\ = E_C^* + \frac{RT}{3F} \ln \left(\frac{1}{[\text{Na}^+]^{3x/2y}[\text{Cl}^-]^{3+3x/2y}} \right) \quad [14]$$

E_A^* , E_C^* , and E^* ($=E_C^* - E_A^*$) are constants under the assumptions made above. According to Ref. 4, $[\text{Cl}^-]_{\text{ref}} = 0.07447M$ at 175°C . From this value the model gives $[\text{AlCl}_4^-]_{\text{ref}} = 8.8747M$, thus $E_A^* = -0.1618\text{ V}$ at 175°C . In Eq. 13, 14, and the following Nernst expressions throughout this paper, concentrations are used instead of activities, and the diffusion potential across the Al_2O_3 -diffusion pin has been ignored. These approximations seem reasonable under our conditions; see Ref. 10 and 11.

By means of Eq. 13 and 14 the cell voltage, E , can be written

$$E = E_C - E_A = E^* + \frac{RT}{3F} \ln \left(\frac{[\text{Cl}^-]}{[\text{AlCl}_4^-][\text{Na}^+]^{3x/2y}[\text{Cl}^-]^{3x/2y}} \right) \quad [15]$$

In Part II experimental coulometric titrations are compared with model calculations based on the general reaction 11, showing that essentially NiCl_2 is formed at the cathode during charging. Therefore during discharging, the general overall cell and cathode reactions can be written as Eq. 16 and 17, respectively



By means of the Nernst law, the corresponding equilibrium potential of the cathode can be expressed as

$$E_C = E_C^* + \frac{RT}{3F} \ln \left(\frac{[\text{Na}^+]^{x/2}}{[\text{Cl}^-]^{(6-x)/2}} \right) \quad [18]$$

From comparison of our coulometric titrations with model calculations based on the general reaction 16, we have found that reduction of NiCl_2 to Ni is associated with consumption of NaCl ; see Part II and below. It is important to note that we cannot determine from our measurements whether $\text{Na}_x\text{Ni}_y\text{Cl}_{2y+x}$ compounds really are formed as intermediates during charging. This is because consumed sodium chloride may simply exist as NaCl crystals in the electrode, isolated from the melt. In fact strong experimental evidence exists that the latter indeed is the case.¹²

Solution of the model equations.—The expressions 2 to 8 together with 11 and 12 cannot be rearranged to a new set

of equations expressing concentrations explicitly as a function of the degree of charge or discharge. Therefore the equations were solved by the following iterative procedure. The concentrations of sodium and, in the general case, of the sulfide species (presuming values for (n, m)) can be calculated directly from starting masses by means of 12, 8, 7 and 6. Equations 4 and 5 are combined and rearranged to new relations expressing $[\text{AlCl}_4^-]$ and $[\text{Al}_2\text{Cl}_7^-]$ as a function of $[\text{Cl}^-]$, $[\text{Al}_2\text{Cl}_6]$, and in the general case also of $[\text{Al}_n\text{S}_{n-1}\text{Cl}_{2n+2-m}^-]$. After calculation of $[\text{AlCl}_4^-]$ and $[\text{Al}_2\text{Cl}_7^-]$, $[\text{Cl}^-]$, and $[\text{Al}_2\text{Cl}_6]$ are calculated by means of 2 and 3, respectively. In the first iteration loop $[\text{Cl}^-]$ and $[\text{Al}_2\text{Cl}_6]$ can be assumed zero. Only a few iteration loops (<15) were necessary in order to obtain concentrations constant within seven significant digits. Finally the equilibrium potentials of anode and cathode can be obtained by means of the Eq. 13 and 14, respectively.

In connection with the analysis of the experimental coulometric titrations (presented in Part II) we have calculated concentrations from measured anode potentials, which was done by a similar iterative procedure.

Calculated equilibrium potentials of the system Al/NaCl-AlCl₃/Ni.—Assuming NiCl_2 formation, values of the anode and cathode potential and cell voltage have been calculated as a function of the melt composition, by means of the model with $x = 0$ and $y = 1$ in Eq. 10-15. The results are shown in Fig. 2. The constant, E_C^* (needed for calculating cathode potentials) was obtained from measured cathode and anode potentials in the following way: first chloride concentrations were calculated by means of the model from the anode potentials given in Part II, Fig. 9, and thereafter Eq. 14 (with the, respective, cathode potentials given in Part II, Fig. 8) was solved for E_C^* . On averaging E_C^* became $0.8761 \pm 0.0005\text{ V}$.

For saturated melts the calculated cell voltage is 0.9765 V , which is in agreement with our experiments, compare Part II, Fig. 3A. Moreover, the curve of the anode potential is in good agreement with the work of Boxall *et al.*¹³

Variation of cathode potential.—The expressions 14 and 18 for the cathode potential are derived by means of the Nernst law, *i.e.*, the variation of the cathode potential is assumed to be caused only by changes in composition of the molten salt. In other words, the compound formed is assumed to be $\text{Na}_x\text{Ni}_y\text{Cl}_{2y+x}$ having a fixed composition independent of the degree of charge or discharge. Equations 14 and 18 can be rewritten as

$$\frac{E_C \cdot F}{R \cdot T} = \frac{E_C^* F}{RT} + \frac{g}{6} \ln ([\text{Na}^+] \cdot [\text{Cl}^-]) - \ln [\text{Cl}^-] \quad [19]$$

where $g = -3x/y$, x for charging and discharging, respectively. $|g|$ is the amount of NaCl consumed by the cathode reaction per 6 moles of electrons transferred.

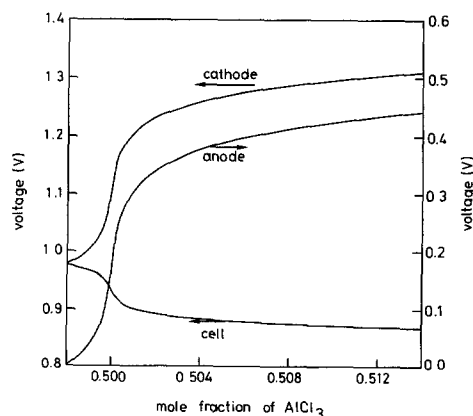


Fig. 2. Calculated thermodynamic potentials of aluminum and nickel electrodes and cell voltages of the system $\text{Al}/\text{NaCl}-\text{AlCl}_3/\text{Ni}$ at 175°C , assuming the positive electrode reaction to be formation/decomposition of NiCl_2 .

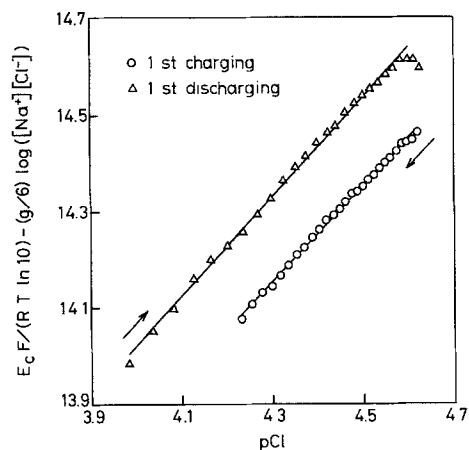
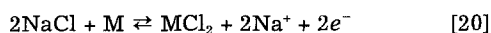


Fig. 3. Measured cathode potentials (normalized as $E_c \cdot F / (R \cdot T \cdot \ln 10) - g/6 \log ([Na^+] \cdot [Cl^-])$, see Eq. 19) plotted vs. pCl and fitted by least-squares regression lines. Sodium and chloride concentrations were calculated from measured anode potentials.

Therefore, the correctness of the assumption of a fixed composition (E_c^\ddagger is constant) can be tested for experimental cells by plotting the quantity $\{E_c \cdot F / (R \cdot T \cdot \ln 10) - g/6 \log ([Na^+] \cdot [Cl^-])\}$ vs. pCl ($= -\log [Cl^-]$). The g values are obtained from model fitting to the experimental curve of the anode potentials. The concentrations of sodium and chloride are calculated from the measured anode potentials, by means of the model. The anode potential is an unambiguous function of the melt composition. If Eq. 14 and 18 are correct expressions, the experimental points should form straight lines with slopes of +1. An example of such a plot is given in Fig. 3, showing charging and discharging together with least-squares regression lines (details on experimental data are given in Part II). Slopes and r^2 correlation coefficients were -0.99 ± 0.01 and 0.9979 for charging and 1.02 ± 0.01 and 0.9972 for discharging. The three last data points measured before termination of discharging were not included in the curve fitting, since the cathode reaction was different during the last three titration periods, as indicated by an increase of the reaction overvoltage from ~ 100 mV (in the main part of discharging) to ~ 500 mV. The close approach to a slope of +1 strongly indicates that the observed variation of the cathode potential solely is caused by changes in the electrolyte, hence E_c^\ddagger is indeed a constant and Eq. 19 is applicable.

This makes it reasonable to depict the experimental data as $E_c \cdot F / (R \cdot T \cdot \ln 10) + \log [Cl^-]$ vs. $\log ([Na^+] \cdot [Cl^-])$, which should fit to straight lines with slopes equal to $g/6$ according to Eq. 19. The consumption of NaCl may thus also be determined from the variation of the cathode potential. If cathode potentials had been measured with accuracies of ca. ± 0.1 mV, it should be possible to derive accurate g values from this plot. Unfortunately in our case the accuracy was ± 1 mV, see Part II. Nevertheless, by means of least-squares linear regression, $|g|$ -values of 0.06 ± 0.05 and 0.15 ± 0.07 were found for charging and discharging, respectively. These figures do agree reasonably well with the $|g|$ -values obtained from model fitting to the anode potential curve, which were 0.0 for charging and 0.30 ± 0.15 for discharging, see Part II. This indicates that $NiCl_2$ is formed directly during charging and that reduction of $NiCl_2$ to Ni is associated with a consumption of NaCl.

Comparison with "Zebra" batteries.—In the so-called "Zebra" batteries,¹⁴ the comparable cathode systems, Fe/ $FeCl_2$ or Ni/ $NiCl_2$, in contact with NaCl saturated $NaAlCl_4$ melts at $\sim 250^\circ C$, are utilized together with a solid ionic conducting tube containing a liquid sodium anode. The overall reaction in these batteries can be written



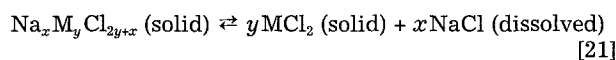
where $M = Fe$ or Ni (Na^+ are supplied or withdrawn via the

solid electrolyte). The capacity is given by the amount of solid NaCl present at the cathode. Excessive Fe or Ni, normally 60–70%,¹⁵ serves as current collector. In our cells, with no excess of NaCl, the corresponding overall reaction is given by Eq. 11 with $x = 0$ and $y = 1$.

For the Fe/ $FeCl_2$ couple, it is known,¹⁶ that the cathode reaction at low loads proceeds via two sequential steps. During the first step the intermediate compound Na_6FeCl_8 is formed, which has been identified by x-ray diffraction analyses.¹⁶ The formation of Na_6FeCl_8 also is manifested as two levels on the open-circuit voltage vs. composition curve with accordingly relative lengths.¹⁷

In the case of Ni/ $NiCl_2$ -“Zebra” cells, charging/discharging proceeds at a single potential level^{9,18,19} (also found in this work). This has been taken to indicate that transformation between Ni and $NiCl_2$ occurs in one step, i.e., that no intermediate compound of the type $Na_xNi_yCl_{2y+x}$ seems to be formed in the Ni/ $NiCl_2$ - $NaAlCl_4$ system.

In general, $Na_xM_yCl_{2y+x}$ -type compounds (M is a transition metal in the divalent state) in contact with molten $NaCl-AlCl_3$, will enter into the displacement equilibria Eq. 21



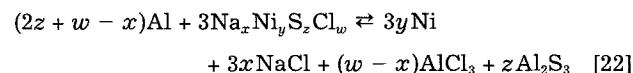
The more acidic the melt, the more favored is the decomposition of $Na_xM_yCl_{2y+x}$ into the assumed insoluble transition metal chloride and soluble NaCl. Therefore, these double salt compounds should be less stable in our cells (with acidic melts) than in the Zebra batteries (with basic melts).

Is $Na_xNi_yCl_{2y+x}$ nevertheless formed?—It is clear from the observed consumption of NaCl, that Na^+ participates in the cathode reaction during discharging. This can be explained by the increased Na^+ activity at the $NiCl_2/NaAlCl_4$ interface during cathodic polarization. Sodium ions and electrons may simply react with $NiCl_2$ forming Ni and NaCl. However, the possibility exists, that the reduction of $NiCl_2$ to Ni proceeds via $Na_xNi_yCl_{2y+x}$ transition state compounds. Reduction via $Na_xNi_yCl_{2y+x}$ may be kinetically more favorable (associated with lower overpotentials) than direct reduction to Ni. The increased Na^+ activity during cathodic polarization contributes to the stabilization of Na^+ rich compounds. Furthermore, several $Na_xFe_yCl_{2y+x}$ compounds, including $FeCl_2$, have very similar crystal structures²⁰ with close-packed layers of chloride. This probably also holds for analogous nickel compounds.^{21,22} Therefore, $Na_xNi_yCl_{2y+x}$ compounds may be formed during cathodic polarization.

As mentioned above, sodium is probably not involved in the cathode reaction during charging. This seems reasonable, since during anodic polarization the chloride activity becomes high at the cathode, favoring direct oxidation of Ni to $NiCl_2$.

Sulfide (Chalcogen) Containing Cells

$Na_xNi_yS_zCl_w$ formation.—Considering the general case, nickel may react with sodium, chloride, and sulfide from the melt forming a $Na_xNi_yS_zCl_w$ compound. Accordingly the overall cell reaction can be formally written as Eq. 22



which causes changes in the composition of the electrolyte according to Eq. 23a through 23c

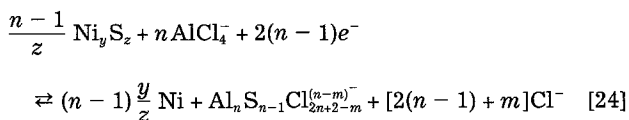
$$n_{NaCl} = n_{NaCl}^0 - \frac{x}{2z + w - x} n_e \quad [23a]$$

$$n_{AlCl_3} = n_{AlCl_3}^0 - \frac{w - x}{3(2z + w - x)} n_e \quad [23b]$$

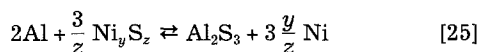
$$n_{Al_2S_3} = n_{Al_2S_3}^0 - \frac{z}{3(2z + w - x)} n_e \quad [23c]$$

Ni_yS_z -formation.—However, when the cell is in the low charge state (i.e., the cell voltage is on the low potential

plateau, No. 1) it can be shown that the cathode reaction involves formation/decomposition of essentially a pure nickel sulfide, see below. The cathode reaction taking place is then



In this case the Eq. 22 and 23 will reduce to Eq. 25 and 26, respectively



$$n_{\text{NaCl}} = n_{\text{NaCl}}^0; \quad n_{\text{AlCl}_3} = n_{\text{AlCl}_3}^0; \quad n_{\text{Al}_2\text{S}_3} = n_{\text{Al}_2\text{S}_3}^0 - n_e/6 \quad [26]$$

n_{NaCl} stays constant since Na^+ is assumed not to be involved in the electrode reactions. n_{AlCl_3} stays constant too, since both the precipitation of Al^{3+} at the anode and the formation of Ni_yS_z is taken into account by means of the last expression in Eq. 26.

The equilibrium potential of the cathode reaction, 24, (relative to the reference electrode) is given by the Nernst law according to relation 27

$$E_c = E_c^* + \frac{RT}{3F} \ln \left(\frac{[\text{AlCl}_4^-]^{3n/2(n-1)}}{[\text{Al}_n\text{S}_{n-1}\text{Cl}_{2n+2-m}^{(n-m)-}]^{3/2(n-1)}[\text{Cl}^-]^{3+3m/2(n-1)}} \right) \quad [27]$$

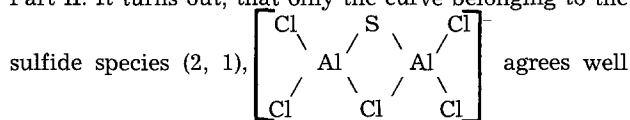
E_c^* is independent of concentrations, but is a function of n , m , and the stoichiometry of the formed nickel sulfide.

The low potential plateau, No. 1, Ni_yS_z formation.—Plateau length.—Plateau No. 1 is only observed for cells containing chalcogenide and is therefore due to formation/decomposition of (in general) an $\text{Na}_x\text{Ni}_y\text{S}_z\text{Cl}_w$ compound. However, from comparison of experimental results with Eq. 23, it can be quantitatively concluded, that plateau No. 1 is associated with essentially a pure nickel sulfide for the following reasons: as shown in Part II, the experimentally obtained lengths of the low potential plateau, No. 1, are in close accordance with a nickel sulfide reaction, in the sense that sulfide from the melt reacts quantitatively in form of S^{2-} with the nickel felt electrode (the compound formed may also contain Na and Cl). This means, according to Eq. 23c, that $w-x \approx 0$ (one can put $z=1$ in Eq. 23 without making the expressions less general), which together with Eq. 23b states that n_{AlCl_3} is approximately constant. It is further observed experimentally (Part II) that the anode potential remains essentially constant along plateau No. 1, which reflects that only minor changes occur in the composition of the electrolyte, and since n_{AlCl_3} is nearly constant the same has to be true for n_{NaCl} . The observed small variation of the anode potential is most probably caused by a change in the concentration of chloride associated with release/uptake of sulfide from the melt and thus not due to a relative change of n_{AlCl_3} compared with n_{NaCl} , see Part II. Therefore, according to Eq. 23a, $x \approx 0$ and consequently $w \approx 0$. This shows, that plateau No. 1 is due to formation/decomposition of essentially a pure nickel sulfide.

Plateau curveform.—Since the low potential plateau, No. 1, is associated with essentially Ni_yS_z , the cathode potential should vary according to Eq. 27. By fitting this equation to the experimental data information can be obtained about the kind of sulfide species present in the melt. However a problem is that E_c^* and (n, m) are unknown. Further, the transition points between cathode low and high potential plateaus (No. 1 and No. 2, see Fig. 1 or Part II, Fig. 10) are known only within a precision given by the finite size of the coulometric steps. Therefore, after assuming a set of n and m (type of sulfide species present in the melt), fitting of the curve-form (calculated by means of Eq. 27) to the experimental data must be done along both the ordinate (E_c^* unknown) and along the abscissa (exact transition points unknown). Model curves were calculated as a function of the type of sulfide species, assuming the cathode reaction to be given by Eq. 24. The initial values

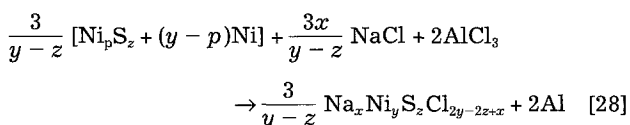
used were 0.1174₀ mole of AlCl_3 , 0.1138₀ mole of NaCl , and zero mole of Al_2S_3 , corresponding to the composition of the experimental melt just before the shift of the cathode potential from the high to low potential plateau (No. 2 to No. 1) during first discharging, see Part II, Fig. 10. Setting the initial molar amount of Al_2S_3 to zero is a good approximation. This is because the voltage change of ~ 0.25 V between the high and low potential plateau (Fig. 10), corresponds to about five decades change in the concentrations of the sulfide species, according to Eq. 27.

The calculated cathode potentials vs. the number of coulombs for different assumed sulfide species are shown in Fig. 4. Since the absolute potentials are unknown, the curves were arbitrarily normalized with an additive constant to 1.020 V at 399.9 coulombs in order to fit into a single figure. Therefore, one should notice the difference in the curve form and not the relative displacement of the curves in the ordinate direction. Fitting of the calculated curves to the experimental titration curves is described in Part II. It turns out, that only the curve belonging to the



with the experimental data, see Part II for further details.

Potential plateau, No. 2.—Experimentally it is observed, that the level of the cathode potential along plateau No. 2 and its variation vs. the number of coulombs strikingly resembles what was obtained for the chalcogenide-free cell. Since only one plateau is observed it should be due to a single compound containing divalent Ni. As a consequence, the formed compound must belong to the series $\text{Na}_x\text{Ni}_y\text{S}_z\text{Cl}_{2y-2x+x}$. The overall cell reaction can in general be written as Eq. 28



corresponding to a transfer of six electrons. Ni_pS_z designates the pure nickel sulfide (most probably Ni_3S_2 as discussed in Part II) presumably formed during the low potential charging range. Obviously, Eq. 28 only makes sense if x , y , z , p , and $y-z$ are non-negative numbers. Allowing nickel metal to participate in reaction 28 requires that $y \geq p$. Since reduction of Ni_pS_z is unlikely, the maximum amount of nickel metal that can be oxidized to the assumed Ni^{II} -compound is three atoms when transferring six electrons, giving the restriction $3(y-p)/(y-z) \leq 3$, which implies that $p \geq z$ (since $y > z$). Totally then, Eq. 29 is obtained

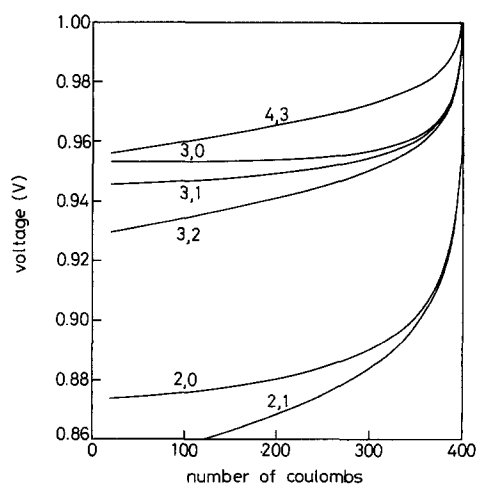
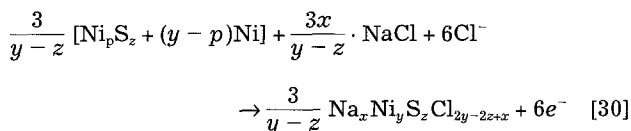


Fig. 4. Calculated cathode potentials for different sulfide species of the type $\text{Al}_n\text{S}_{n-1}\text{Cl}_{2n+2-m}^{(n-m)-}$, designated by (n, m) in the figure. Cathode reaction and potential are given by Eq. 25 and 27, respectively.

$$y \geq p \geq z \geq 0 \quad [29]$$

Reaction 28 terminates when either all Ni-metal or all Ni_pS_z is consumed (NaAlCl_4 is assumed to be present in excess). Which of the two reactants becomes limiting depends on the relative consumption of Ni metal and Ni_pS_z in reaction 28 and on the relative amounts of these compounds in the cell.

The cathode reaction belonging to the overall reaction 28 is given in Eq. 30



By means of the Nernst equation, the equilibrium cathode potentials can be expressed as Eq. 31

$$E_c = E_c^* + \frac{RT}{3F} \ln \left\{ \frac{1}{[\text{Na}^+]^{3x/(2y-2z)} [\text{Cl}^-]^{3+(3x/(2y-2z))}} \right\} \quad [31]$$

In Part II model calculations based on Eq. 28 are tested against the experimental variation of cathode and anode potential.

Summary and Conclusion

This work presents a model describing thermodynamic properties of Al/NaCl-AlCl₃-Al₂X₃/Ni-felt (X = S, Se, Te) batteries with basic to slightly acidic melts, and the corresponding system without chalcogen. The model consists of a set of equations describing the concentrations of the species in the melt as a function of the overall composition of the melt specified by the mole fractions of the formal species NaCl, AlCl₃ and Al₂X₃. Further the model contains (i) equations specifying the changes in the overall composition of the melt caused by assumed electrode reactions and (ii) expressions specifying the equilibrium potentials of the electrodes as a function of the melt composition. These sets of equations were solved by iterative numerical methods.

For cells without chalcogen, curves were calculated showing the variation of anode potential, cathode potential, and cell voltage as a function of electrolyte composition under the assumption of NiCl₂-formation. Reduction of NiCl₂ to Ni was found to be associated with a consumption of NaCl.

For chalcogen (sulfide) containing cells, modeling was performed on both plateau No. 1 and plateau No. 2.

For plateau No. 1, curves were calculated for different assumed sulfide species showing the variation in the cathode potentials vs. degree of charge. In Part II these curves are fitted to experimental data in order to determine the sulfide species present in slightly acidic melts.

A general equation is proposed for the reaction taking place along plateau No. 2 assuming $\text{Na}_x\text{Ni}_y\text{S}_z\text{Cl}_{2y-2z+x}$ formation. Calculated charging curves based on this general reaction are fitted to experimental data in Part II.

Acknowledgments

We wish to thank Torben Jacobsen for valuable discussions and the Danish Ministry of Energy, Thomas B.

Thriges Fond, the Danish Technical Science Research Council, and the Technical University of Denmark for financial support.

Manuscript submitted Aug. 8, 1992; revised manuscript received Aug. 20, 1993.

REFERENCES

- H. A. Hjuler, R. W. Berg, and N. J. Bjerrum, *Power Sources*, **10**, 1 (1985); (Proceedings from the 14th International Power Sources Symposium 1984, Brighton, England).
- R. Marassi, G. Mamantov, and J. Q. Chambers, *This Journal*, **123**, 1128 (1976); R. Marassi, G. Mamantov, M. Matsunaga, S. E. Springer, and J. P. Wiaux, *ibid.*, **126**, 231 (1979).
- K. A. Paulsen and R. A. Osteryoung, *J. Am. Chem. Soc.*, **98**, 6866 (1976); J. Robinson, B. Gilbert, and R. A. Osteryoung, *Inorg. Chem.*, **16**, 3040 (1977).
- H. A. Hjuler, A. Mahan, J. H. von Barner, and N. J. Bjerrum, *ibid.*, **21**, 402 (1982).
- P. B. Brekke, J. H. von Barner, and N. J. Bjerrum, *ibid.*, **18**, 1372 (1979).
- R. W. Berg, S. von Winbush, and N. J. Bjerrum, *ibid.*, **19**, 2688 (1980).
- R. W. Berg, H. A. Hjuler, and N. J. Bjerrum, *J. Chem. Eng. Data*, **28**, 253 (1983).
- B. C. Knutz, R. W. Berg, H. A. Hjuler, and N. J. Bjerrum, *This Journal*, **140**, 3380 (1993).
- R. J. Bones, D. A. Teagle, S. D. Brooker, and F. L. Cullen, *This Journal*, **136**, 1274 (1989).
- J. H. von Barner and N. J. Bjerrum, *Inorg. Chem.*, **12**, 1891 (1973).
- G. Torsi and G. Mamantov, *ibid.*, **10**, 1900 (1971).
- B. V. Ratnakumar, A. I. Attia, and G. Halpert, *J. Power Sources*, **3**, 385 (1991).
- L. G. Boxall, H. L. Jones, and R. A. Osteryoung, *This Journal*, **120**, 223 (1973).
- R. M. Dell and R. J. Bones, in *Proceedings of 22nd International Energy Conversion Engineering Conference*, pp. 1072-1077, Philadelphia, PA, Aug. 1987.
- R. J. Bones, D. A. Teagle, and S. D. Brooker, *Power Sources*, **12**, 537 (1989); (Proceedings from the 16th International Power Sources Symposium 1988, Bournemouth, England).
- N. D. Nicholson, D. S. Demott, and R. Hutchings, *Power Sources*, **12**, 549 (1989); (Proceedings from the 16th International Power Sources Symposium 1988, Bournemouth, England).
- R. J. Bones, D. A. Teagle, S. D. Brooker, F. L. Cullen, and J. Lumsdon, Abstract 553, p. 786, The Electrochemical Society Extended Abstracts, Vol. 87-1, Philadelphia, PA, Meeting, May 10-15, 1987.
- B. V. Ratnakumar, A. I. Attia, and G. Halpert, in *34th International Power Sources Symposium*, p. 17, sponsored by The Institute of Electric and Electronics Engineers Industry Application Society and The U.S. Army Laboratory Command Electronics Technology and Device Laboratory, Power Sources Division, Cherry Hill, NJ, June 25-28, 1990.
- B. V. Ratnakumar, S. Di Stefano, and G. Halpert, *This Journal*, **137**, 2991 (1990).
- K. T. Adendorft and M. M. Thackeray, *ibid.*, **135**, 2121 (1988).
- H. D. Lutz, P. Kuske, and K. Wussow, *Z. Anorg. Allg. Chem.*, **553**, 172 (1987).
- A. Ferrari, A. Braibanti, and G. Bigliardi, *Acta Cryst.*, **16**, 846 (1963).